

Engineering
Mechanical Engineering fields

Okayama University

Year 2003

A miniature inspection robot negotiating
pipes of widely varying diameter

Koichi Suzumori
Okayama University

Shuichi Wakimoto
Okayama University

Masanori Tanaka
Okayama University

This paper is posted at eScholarship@OUDIR : Okayama University Digital Information
Repository.

http://escholarship.lib.okayama-u.ac.jp/mechanical_engineering/17

A Miniature Inspection Robot Negotiating Pipes of Widely Varying Diameter

Koichi SUZUMORI, Shuichi WAKIMOTO, and Masanori TAKATA

Okayama University, Japan

suzumori@sys.okayama-u.ac.jp

Abstract

The purpose of this research is to realize a small robot which can negotiate pipes whose diameter varies widely during the robot's course. A new in-pipe locomotion mechanism named "snaking drive" is proposed in this paper and its potential and fundamental characteristics are shown with experimental data of the prototype model.

First, in the sections 2 to 5, the basic traveling characteristics of the snaking drive mechanism are discussed: a theoretical formula of the fundamental characteristics and control algorithm are derived, the motions of the robot are simulated on a PC, and the prototype model was designed, developed, and tested.

Next, in the sections 6 and 7, additional control algorithms for the front link are derived. They are necessary for steering at T-branches and L-bends of pipes, and also for camera view stabilization. Their performances are also shown by software simulation and experiments.

The prototype robots moved in pipes whose diameter varies between 55mm to 331mm with the maximum speed of 22 mm/s. The paper also shows that the prototype negotiates T-branches and L-bends of pipes with inspection capability through a camera mounted on the robot.

1. Introduction

Although various pipe inspection robots have been developed [1-6], there is almost no robot which can negotiate pipes of changing diameters. The diameters of a pipe can often change during the robot's course in practical plants and gas/water supply lines. And there can also be sediment or other debris obscuring the robot's path. Therefore, realization of a robot capable of negotiating pipes of varying diameter has been a practical and very important subject.

The final goal of this research is to realize a small robot which can negotiate pipes of diameter 1 to 6 inches, which are very popular in practical plants and also difficult to be inspected inside using conventional machines. The authors experimented with a new locomotion mechanism named "snaking drive". This paper shows the potential of the mechanism theoretically and experimentally.

2. Driving Principle

Several types of snake-like mobile robots have been developed [7-9]. They have the potential to offer good mobility on various spaces, such as narrow paths and on a plane.

One of the authors has applied a snake-like traveling method to an in-pipe locomotion robot using pneumatic rubber actuators and showed the potential to travel in pipes of widely varying diameter [8]. Snaking drive mechanism reported in this paper is basically based on the former mechanism and is designed and developed to be more practical and to have better adaptability to pipe diameter by increasing the degree of freedom of the robot and by using rigid link mechanisms and power micro DC motors.

Figure 1 shows a configuration and a driving sequence of the snaking drive mechanism. The robot shown in Fig. 1 consists of six links which are connected serially by rotational joints. The joints are driven by sine wave signals with small phase differences between adjoining joints. This algorithm is shown by the following equation;

$$R(i) = A \sin \left\{ \omega t - 2\pi \frac{(i-1)}{\lambda} \right\} \quad (1)$$

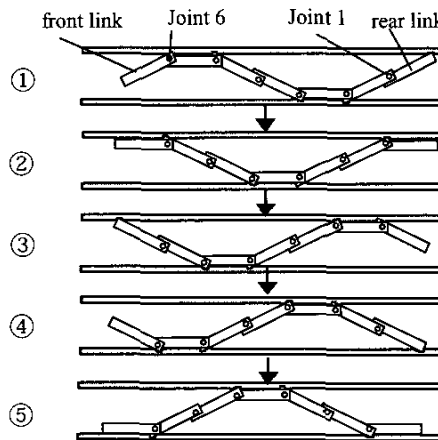


Figure 1 Driving principle of snaking drive

where i represents the identify number of the joint, numbered from the rear to the front of the robot, $R(i)$ represents the reference value of the bending angle of the i -th joint. A , ω , and t represent the amplitude of the bending angle, the angular frequency, and time, respectively. λ represents the number of links forming one wave, which is named wave length.

Figure 1 shows an example of driving sequence, where the number of the joints, n is 6, the wave length, λ is 6, (six links forms one sine wave), and the phase difference between the adjoining joints is $\pi/3$ [rad].

Snake-like movement caused by this algorithm makes the robot move in the direction of the delayed phase link as shown in Fig.1 using the friction between the robot and the pipe wall.

There are many options of control and mechanical design parameters. Effects of the optional parameters to robot mobility are discussed in the following sections.

3. Theoretical characteristics

Kinematical considerations lead theoretical characteristics and control algorithms of the snaking drive mechanism. In this report, the width of the links is not considered for simplicity.

3.1 Optimization of the amplitude of the bending angle

Optimal amplitude of the bending angle, A is obtained as a function of the pipe inner diameter, D . Figure 2 shows an example of analysis for $\lambda=6$. Kinematical consideration based on Fig.2 leads the following equations;

$$\begin{aligned} \theta_1 = \theta_4 = 0 \\ \theta_2 = \theta_3 = -\theta_5 = -\theta_6 = A \\ D = |2L \sin(\theta_2)| \end{aligned} \quad (2)$$

where D and L represent the pipe inner diameter and the length of the link, respectively. θ_i represents the bending angle of the i -th joint.

Optimal amplitudes for $\lambda=4$ and 8 are also obtained in similar ways. The results are shown in Fig. 3.

3.2 Traveling velocity

The traveling velocity of the robot in pipes is also

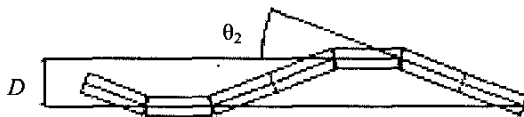


Figure 2 Theoretical analysis between pipe inner diameter and bending angle ($\lambda=6$)

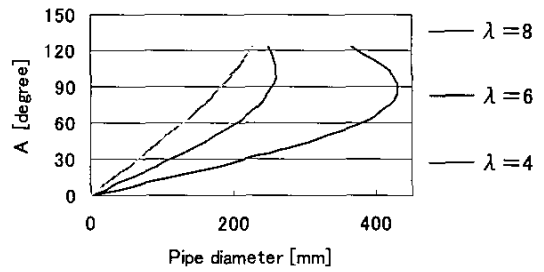


Figure 3 Optimal amplitudes of bending angle

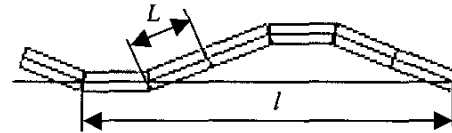


Figure 4 Theoretical analysis of travelling velocity of the robot ($\lambda=6$)

obtained theoretically as a function of the pipe inner diameter. Define the speed parameter of v as the traveling distance caused during a snaking cycle, or $2\pi/\omega$. Thus, the parameter v has the dimension of mm/cycle.

Figure 4 shows an example of analysis in the case of $\lambda=6$, where l represents the length of a sine wave of the robot measured in the axial direction. Figure 4 leads the following equation.

$$\begin{aligned} l &= \sum_{n=0}^5 |L \cos \theta'_i| \\ \theta'_2 = \theta'_5 &= 0 \\ |\theta'_0| = |\theta'_1| = |\theta'_3| = |\theta'_4| &= |\theta_2| \\ v &= 6L - l \end{aligned} \quad (3)$$

where θ'_i represents an angle between the $(i+1)$ th link and pipe axis. L represents the link length.

The traveling velocities for $\lambda=4$ and 8 are also obtained in similar ways. The analytical results are shown in Fig. 5.

4. Software simulation of traveling in straight pipes

Simulation using a dynamic mechanical simulator, Working Model was carried out to verify the basic performances of this mechanism as shown in Fig. 6.

Figure 6 shows a robot traveling right to left, from big to small pipe. The robot was found to move successfully

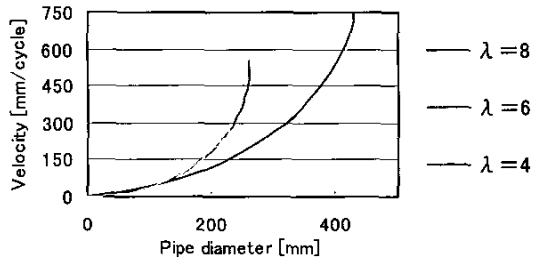


Figure 5 Theoretical travelling velocity

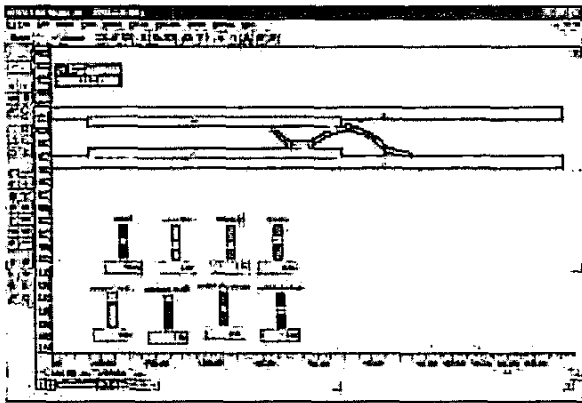


Figure 6 An example of simulation

in pipe, 1 to 6 inch in inner diameter and also to negotiate T-branches and L-elbows.

5. Prototype design and experiments

A prototype robot which moves on two dimensional planes was designed and experimented in order to verify the potential of the snaking drive mechanism. The prototype consists of seven links which are connected serially by six rotational joints.

Figure 7 shows the dimension of the link and Fig. 8 shows the joint structure. Each joint consists of a DC electrical motor, a rotational potentiometer, and a reduction gear with 1/300 reduction ratio. The distance between the joints is 110 mm and the prototype robot is 810 mm long in total. A link weights 50 g and the robot weights 780 g in total.

Experiments were made by traveling the robot between two walls as shown in Fig. 9. The experimental results and theoretical results of the robot velocity are shown in Fig. 10. The frequency was set to be 0.2 cycle/second, which leads the maximum velocity of 22 mm/s..

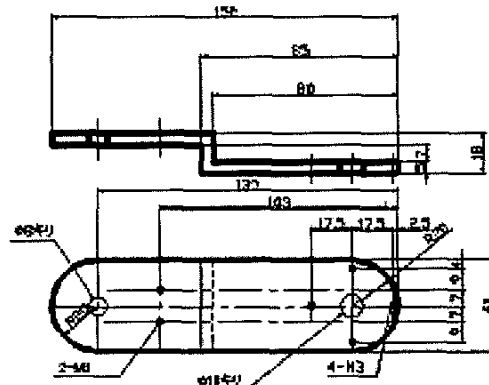


Figure 7 Link dimensions

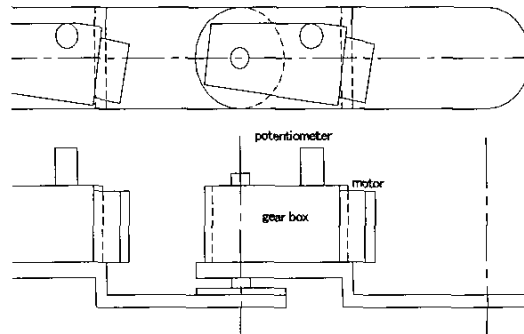


Figure 8 Joint structure of the prototype

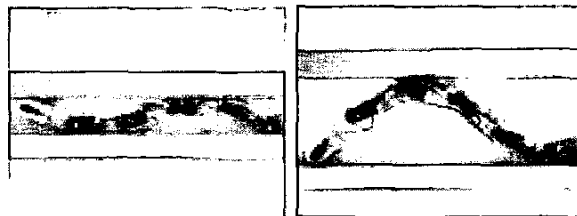


Figure 9 Prototype robot

Distance between walls is 80mm (left) and 200 mm (right)

The distance between the walls was changed from 50 mm to 320 mm and the robot travels successfully between them. The experimental results and theoretical results agree well for the walls-distance of 50 mm to 150 mm. Errors between the experimental results and theoretical results come from the delay of the joint motor response.

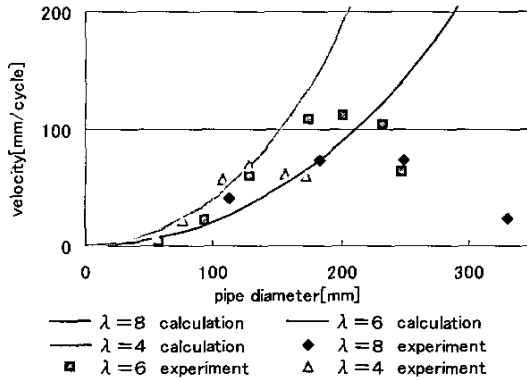


Figure 10 Traveling velocity of the robot (experimental and theoretical results)

6. Additional control algorithm for the front link

Control of the front link of the robot is especially important for stabilization of TV image from the camera mounted on the front of the robot and for steering at pipe branches. For those purposes, additional control algorithms are necessary for the front link.

6.1 Stabilization of camera orientation

The front link is required to keep its orientation constant to stabilize camera images. An algorithm for $\lambda=6$ is obtained geometrically from Fig. 11 as $\theta_2 = -\theta_6.0$

Equation (1) leads the bending angles $R(2)$ and $R(6)$ as follows;

$$R(2) = A \sin \left(\omega t - \frac{\pi}{3} \right) \quad (4)$$

$$R(6) = A \sin \left(\omega t - \frac{5\pi}{3} \right) \quad (5)$$

Then, the bending angle of the joint 6 must be $R'(6)$ as shown below in order to keep camera orientation constant.

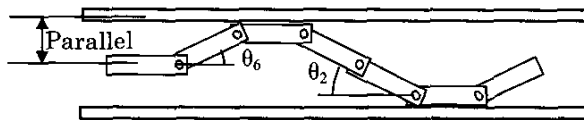


Figure 11 Stabilization control of the camera

$$R'(6) = R(6) + R(2) = A \sin \omega t \quad (6)$$

6.2 Simulation of camera view stabilization

Figure 12 shows a simulation result of the camera stabilizing control. The results show the camera orientation was kept almost constant and the algorithm works well.

6.3 Steering at pipe branches

To negotiate pipe branches and elbows, it is effective to add an offset angle to each joint except the front joint. This means adding an offset θ_{ir} to equation (1) as follows.

$$R''(i) = A \sin \left(\omega t - 2\pi \frac{i-1}{\lambda} \right) + \theta_{ir} \quad (7)$$

for $i=1,2,3,4,5$

The front link must be controlled independently to select the paths at pipe branches. This is described as

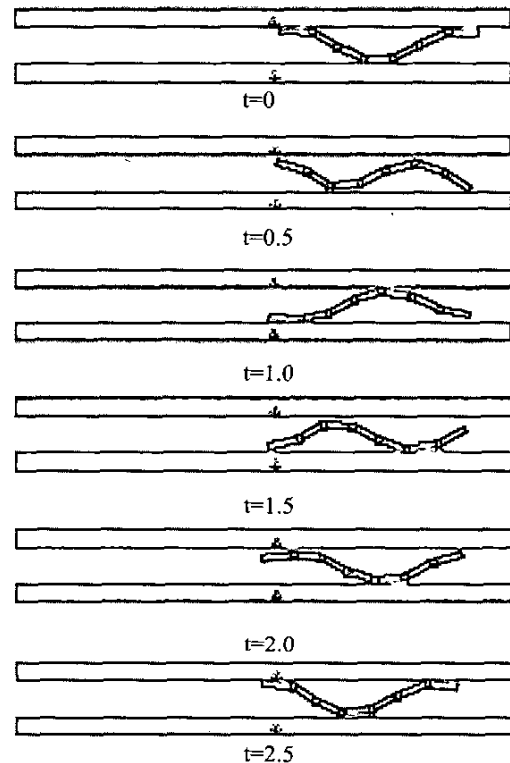


Figure 12 Simulation of Camera stabilizing control

follows;

$$R''(6) = A \sin \omega t + \theta_{6r} \quad (8)$$

6.4 Simulation of negotiating T-branch

A simulation of T-branch negotiation is shown in Fig. 13. Each joint is controlled according to equations (7) and (8). The bending angle of the front joint θ_{6r} is controlled manually using a control bar on a PC display.

As shown in Fig. 14, the orientation of the front link is kept constant and also the robot can be easily control to move in desired path.

7. Experiments

The experiments of camera stabilizing and branch-negotiating were carried out using the prototype model shown in Section 5.

Figure 14 shows an experiment of camera stabilizing.

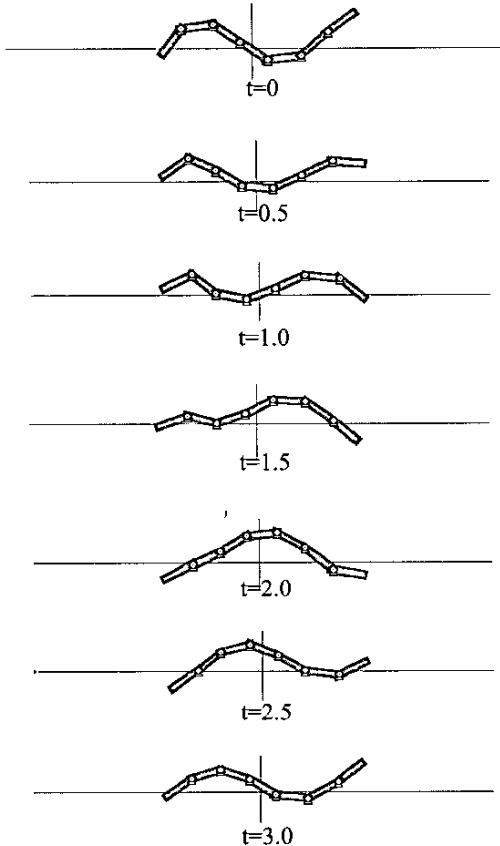


Figure 13 Simulation of robot steering at branches

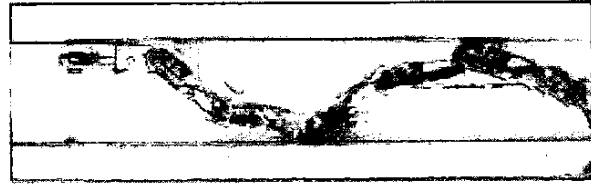


Figure 14 Camera orientation control

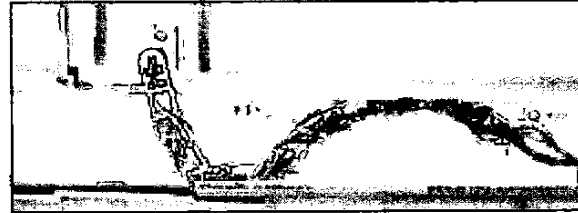


Figure 15 Steering control at T-branch

It was found the camera stabilization works well, while some camera image shakes still remain, which results from backlash of the gears and the friction between the robot and the pipe walls.

T-branch negotiating experiments were made in plastic pipes, 120 mm in diameter as shown in Fig.15. The additional control parameters of the joint bending angle, θ_{ir} is controlled manually by an operator observing the robot and handling a joystick and buttons on a control pendant. In this experiment, the additional bending angle of the joints 1 to 5, $\theta_{1r} \sim \theta_{5r}$ are set to be equal while the additional angle for the 6 th joint is controlled independently.

The robot offers good mobility; the robot can move easily in desired directions with manual control.

The robot was found to negotiate also short elbow pipes.

8. Conclusions

A new mobile mechanism in pipes is proposed and its performances are shown experimentally using a prototype robot. This mechanism is especially effective traveling in pipes with diameter-change.

This paper shows:

- (1) The prototype robot can travel easily in pipes, 55mm to 331 mm in inner diameter. The maximum traveling rate is found to be 22mm/s in pipe 202 mm in inner diameter.
- (2) A new control algorithm for camera view stabilizing was developed. The experiment shows that this algorithm works well.
- (3) The prototype robot negotiates T-branches and L-elbows successfully.

A practical model is now being developed.

Acknowledgment

This work is supported by Electric Technology Research Foundation of Chugoku and Japan Institute of Construction Engineering.

References

- [1] K.Suzumori et al., "Micro inspection robot for 1-in pipes", IEEE/ASME Trans. on Mechatronics, Vol.4, No.3, September 1999, pp.286-292.
- [2] J. Hollingum, "Robot explore underground pipes", Ind.Robot, vol. 25, no.5, pp.321-325, 1998.
- [3] T. Idogaki et al., " A prototype model of micro mobile machine with piezoelectric driving force actuator", Proc. IEEE 6th Int. Symp. Micro Machine and Human Sciences, 1995, pp.193-198.
- [4] T.Fukuda et al., "Giant magnetostrictive alloy (GMA) applications to micro mobile robot as a micro actuator without power supply cables", Proc. IEEE Int. Workshop Micro Electro Mechanical Systemx, Jan. 1991, pp.210-215.
- [5] M. Takahashi et al., "The development of an in-pipe microrobot applying the motion of an earthworm", Proc. IEEE 5th Int. Symp. Micro Machine and Human Sciences, 1994, pp.35-40.
- [6] S.Iwashita, et al., "Development of in-pipe operation micro robots", Proc. IEEE 5th Int. Symp. Micro Machine and Human Sciences, 1994, pp.41-45.
- [7] K.Suzumori and T. Abe, "Applying a flexible microactuators to pipeline inspection robots", Proc. IMACS/SICE Int. Symp. Robotics and Manufacturing Systems, North-Holland, The Netherlands, 1993, pp.515-520.
- [8] S.Hirose, Biologically Inspired Robots (Snake-like Locomotor and Manipulator), Oxford University Press, (1993).
- [9] M. Nunobiki, et al., "An Investigation of Mobility of Inchworm-Type Robot", Proc. France-Japan Congress of Mechatronics, pp.113-118 (2002)